IEEE Access
Multidisciplinary | Rapid Review | Open Access Journal

Received August 22, 2019, accepted September 12, 2019, date of publication September 27, 2019, date of current version October 9, 2019.

Digital Object Identifier 10.1109/ACCESS.2019.2944147

Wideband Spectrum Sensing Based on Bidirectional Decision of Normalized Spectrum for Cognitive Radio Networks

PEIHAN QI[1,2], YI DU[1], DANYANG WANG[1], AND ZAN LI[1], (Senior Member, IEEE)

[1]State Key Laboratory of Integrated Service Networks, Xidian University, Xi'an 710071, China
[2]Key Laboratory of Dynamic Cognitive System of Electromagnetic Spectrum Space, Ministry of Industry and Information Technology, Nanjing University of Aeronautics and Astronautics, Nanjing 211106, China

Corresponding author: Danyang Wang (dywang@xidian.edu.cn)

This work was supported in part by the China Postdoctoral Science Foundation under Grant 2018M631122 and Grant 2019M653558, in part by the National Natural Science Foundation of China under Grant 61901328, and in part by the Key Laboratory Foundation of Ministry of Industry and Information Technology under Grant KF20181912.

ABSTRACT Cognitive radio (CR) is considered to be an effective approach to eliminate the dilemma of spectrum shortage. To meet the ever-increasing demands of instant and accurate spectrum sensing in CR with wideband and multi-frequency-slots, a novel wideband spectrum sensing algorithm based on bidirectional decision of normalized spectrum (BDNP) is proposed in this paper. The proposed algorithm takes the normalized power spectrum within the frequency slot as the detection statistics, and finds out all of the occupied frequency slots in the range of the target bandwidth by searching forward and backward in sequence. The asymptotic normality and independence of Fourier transform is proved firstly, and based on which the false alarm probability of single decision is derived. Additionally, the closed-form expression of decision threshold is obtained by using Neyman-Pearson criterion. Theoretical analysis and simulation results show that the BDNP algorithm can accurately identify occupied frequency slots, which provides the base of avoiding interference to the primary users. Furthermore, comparing with the spectrum sensing algorithm based on conventional spectral estimation (CSE), BDNP algorithm can effectively overcome noise uncertainty in spectrum sensing.

INDEX TERMS Cognitive radio, spectrum sensing, spectrum access, spectrum management, noise uncertainty.

I. INTRODUCTION

With the boosting growth of mobile wireless applications, mobile data traffic is expected to reach 48.3 EB (one billion GB) per month by 2021 [1]. The dramatic increase in wireless radio services results in a huge shortage of authorized spectrum resources [2], [3]. To tackle this problem, cognitive radio (CR) has been widely applied to overcome the contradiction between the demand of wireless access and the scarcely available spectrum resources [4], [5]. Recently, Long-term-evolution-unlicensed (LTE-U) has been designed to execute a sub-band clear assessment (CCA) before accessing the sub-band and transmits when the sub-band is idle. It aims to share the spectrum with other networks such as WiFi and uses the unlicensed spectrum around 5GHz more effectively [6], [7]. Cognitive frequency hopping technique detects the occupancy of the spectrum usage firstly, and then constructs a new architecture of frequency hopping system on the basis of the occupancy status of frequency slots by selecting optimal system parameters to adjust the frequency hopping communication system [8], [9]. It can achieve the avoidance of interference signals and the maximal utilization of spectrum resources. Hence, spectrum sensing [10]–[12], which can distinguish the existence of primary users (PUs) or interference, is the fundamental technique to enable CR. With the explosive growth of wireless applications requiring high rates, wideband spectrum sensing (WSS) emerges to find more available spectrum for the accessible opportunities of tremendous wireless applications [13]–[17]. Moreover, instant and detailed spectrum

The associate editor coordinating the review of this manuscript and approving it for publication was Rui Wang.

sensing on the target frequency band has been featured as the key technique to the seamless connection between the cognitive radio and wireless communications.

In existing literatures, the commonly used real-time spectrum sensing algorithms for multi-signal in wideband can be divided into three categories: quickest sequential search algorithm [18], [19], distributed multi-user sensing algorithm [20]–[23] and wideband multi-signal sensing algorithm based on spectral estimation [24]–[27]. When using the quickest sequential search algorithm [18], [19] for spectrum sensing, the frequency band of interest is divided into a number of subbands, and secondary users acquire the time-domain samples from each subband one by one to determine the existence of primary users. It requires a superheterodyne receiver for multiple mixing or digital filter bank for narrowband filtering to obtain the signal samples when applying this algorithm to the CR networks with wide bandwidth and narrow frequency slots, which leads to highly complex hardware platform and poor real-time performance. Distributed collaborative multi-user sensing algorithms [20]–[22] require each sensor node (SN) transmit the spectrum sensing information to the fusion center, which comprehensively explores the data uploaded by each node to accurately locate the spectrum hole in the frequency domain or the spatial domain. The decision results are more reliable than a single cognitive node, while this algorithm will increase the additional networking as well as communication overhead, and it is not applicable to the CR networks with relatively independent and autonomous node functions, because it may incur high latency due to distributed data fusion, especially when the number of SNs is large. In [23], to solve the problems of the additional overhead and the distributed data fusion, L. Chen *et al.* proposed a cooperative wideband spectrum sensing scheme using over-the-air computation, which utilizes the superposition property of wireless channel to implement the summation of Fourier transform and compute the target fusion directly. Wideband multi-signal sensing algorithm based on spectral estimation is more widely studied. According to different methods and types of spectral estimation, it can be divided into conventional spectral estimation based spectrum sensing [24]–[26] and compressed sensing based ultra-wideband spectrum sensing algorithm [27], [28]. The spectrum sensing algorithm based on conventional spectral estimation uses classical methods such as the periodogram to calculate the power spectrums of the received signals, which are divided into subbands with equal bandwidth for comparing the subband powers with the predetermined threshold to detect the occupancy status of the frequency slots, hence this algorithm is simple to implement and to detect multiple signals that do not overlap with each other in frequency. E. H. Salman *et al.* proposed a discrete cosine transform periodogram based spectrum sensing scheme applied on both DVB models for AWGN channel and various SNR values, which has a good performance for ten secondary users and low SNR [24]. N. Wang *et al.* proposed an optimal threshold setting algorithm based on Welch's periodogram to adapt to the sensing of OFDM signals at the low SNR levels [25]. But the performance of conventional spectral estimation based spectrum sensing is sensitive to the noise uncertainty because of taking the subband power as the test statistic [26]. In [27], A. Taherpour *et al.* proposed a generalized likelihood ratio detector for multiple secondary users (SUs) to overcome noise uncertainty in spectrum sensing. On the other hand, the ultra-wideband spectrum sensing algorithm based on compressed sensing can break the constraints of the Nyquist sampling theorem, digitalizing the ultra-wideband signal at a relatively lower sampling rate, and recovering Fourier transform of the signals with a relatively higher probability while limiting the recovering error in a very low level, and then obtaining the power spectrum of signals and achieving ultra-wideband multi-signal spectrum sensing. H. Qi *et al.* presented a two-dimensional (2-D) compressive spectrum sensing scheme by applying compression in both frequency and spatial dimensions in pursuit of compressive sampling further beyond Nyquist rate and better recovery performance [28]. Y. Ma *et al.* proposed a blind sub-Nyquist cooperative wideband spectrum sensing scheme to reduce energy consumption in wideband signal processing without loss of performance [29]. However, this algorithm requires high sparsity in signal and high signal-to-noise ratio, and the noise folding caused by compressed sampling [30] brings $3dB$ loss in recovery signal-to-noise ratio when doubling the compression ratio.

In this paper, we propose a spectrum sensing algorithm based on bidirectional search of normalized spectrum (BDNP), which takes the normalized power spectrum as the test statistic. The proposed algorithm first performs the forward decision to search the frequency slot that its normalized power spectrum is greater than the forward threshold γ_{max}. If no frequency slot was found in the forward search, the backward decision is performed to find the frequency slot with its normalized power spectrum less than the backward threshold γ_{min}. Once a frequency slot is found in a single bidirectional search, which means this slot is occupied, then it will be taken out of the frequency bands, and the normalized power spectrum of the rest frequency slots will be recalculated for the next bidirectional searches until all occupied frequency slots are found. The closed form of the forward and backward decision threshold can be obtained using Neyman-Pearson criterion, which makes this algorithm independent of the noise variance. The computational complexity of this algorithm is low, which makes real-time wideband multi-signal spectrum sensing possible. The simulation results show that the proposed algorithm is able to effectively overcome the influence of noise uncertainty on spectrum sensing performance, and achieve a low false alarm probability and a high detection probability in a wide range of signal-to-noise ratio to complete the in-band multi-signal sensing.

The rest of this paper is organized as follows: Section II presents the system model. The BDNP algorithm is given in Section III. Section IV proposes the closed-form expression of the false alarm probability and the decision

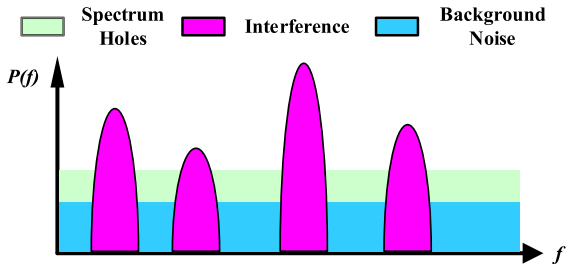

FIGURE 1. The schematic diagram of spectrum holes and interference.

threshold for a single decision, and the upper and lower bounds of the false alarm probability of the BDNP algorithm. Section V shows the discussion and simulation results. Finally, Section VI concludes this paper.

II. SYSTEM MODEL

A. SPECTRUM SENSING MODEL IN COGNITIVE RADIO SYSTEMS

In cognitive radio systems, secondary users monitor the licensed frequency bands that primary users may access, and then use idle subbands to transmit information. If primary users restart information transmissions in the idle subbands, secondary users switch to other idle subbands, or stay in the current subband but change its transmitting power or modulation to avoid interference to primary users. Therefore, CR users first monitor the entire frequency hopping bandwidth before transmitting frequency hopping signals, and sense the occupancy status of frequency slots, which will be used as constraint conditions to generate new CR frequency hopping patterns that exclude the interfered frequency slots and make full use of spectrum holes in interference environments for data transmission. The spectrum holes and interference in wide bands are shown in Fig.1.

In order to establish reliable communication links, CR users first perform spectrum sensing in the frequency band of interest, and the received signals [31] can be expressed as:

$$x(t) = \begin{cases} w(t), & H_0 \\ h(t)\,s(t) + w(t), & H_1 \end{cases} \tag{1}$$

where $x(t)$ is the signal at the secondary-user receiver, $w(t)$ is the additive noise, $h(t)$ is the channel coefficient, and $s(t)$ is the signal that maybe transmitted by one primary user or multiple primary users. When the transmitted signal passes through the AWGN channel, $h(t)$ is a constant. When passing through a flat slow fading channel, $h(t)$ is a complex random variable. Since CR users are concerned about the occupancy of frequency slots, rather than the accurate number of primary users in the frequency hopping wideband, we can regard $s(t)$ as an unknown certain signal. Assuming that $w(t)$ is a complex Gaussian process with a mean of zero and a power spectral density of σ_0^2 and $w(t) = w^r(t) + jw^i(t)$, where $w^r(t)$ and $w^i(t)$ are independent and identically distributed (i.i.d.) Gaussian random variables with a mean of zero and a power spectral density of $\sigma_0^2/2$, H_0 indicates that primary users do not exist in the frequency hopping bandwidth, which means the frequency slots are all idle, while H_1 indicates that there is at least one primary user existing in the frequency hopping bandwidth.

B. STATISTICAL CHARACTERISTICS OF THE POWER SPECTRUM

Without loss of generality, we discuss the statistical characteristics of the power spectrum when $h(t) = 1$ (under the AWGN channel). The received signal of a CR user is converted into digital sequence $x(n), n = 0, 1, \cdots$, through an analog-to-digital converter, and its statistical property is given by

$$x(n) : \begin{cases} N\left(0, \sigma_0^2\right), & H_0 \\ N\left(s(n), \sigma_0^2\right), & H_1 \end{cases} \tag{2}$$

In the hypothesis H_1, $x(n)$ is a Gaussian process with a mean of $s(n)$, and $s(n), n = 0, 1, \cdots$ is a sequence of digital samples of $s(t)$. The N-point samples are successively obtained from $x(n)$, and equally divided into T frames with each sample frame length M. The periodogram estimation of each segmentation can be further expressed as:

$$S_t(k) = \frac{|X_t(k)|^2}{M} = \frac{\left(X_t^r(k)\right)^2 + \left(X_t^i(k)\right)^2}{M} \tag{3}$$

where $k = 0, 1, \cdots, M\text{-}1, t = 1, \cdots, T$.

In order to analyze the statistical characteristics of the periodogram spectral estimation of the signal received by the CR users, two lemmas are first given.

Lemma 1: The Fourier transform $X_t(k)$ has asymptotic normality and mutual independence [32], [33]. a) If Fourier transform of a signal transmitted $P(k)$ by a primary user is determined, $X_t(k)$ obeys the complex Gaussian distribution. b) Fourier transform data $X_t(k)$ and $X_t(k')$ are independent with each other, where $t = 1, \cdots, T, k, k' = 0, \cdots, M\text{-}1, k \neq k'$. c) Fourier transform data $X_t(k)$ and $X_t'(k)$ are independent with each other, where $k = 0, \cdots, M\text{-}1, t, t' = 1, \cdots, T, t \neq t'$.

Lemma 2: Continuous functions of mutually uncorrelated random variables are uncorrelated [34].

It is known from the property a) of **Lemma 1** that $X_t(k)$ obeys the complex Gaussian distribution. Since the DFT is a linear transformation, the real part $X_t^r(k)$ and the imaginary part $X_t^i(k)$ of $X_t(k)$ obey the independent Gaussian distribution, and the probability distribution functions are [35]:

$$X_t^r(k) : \begin{cases} N\left(0, M\sigma_0^2/2\right), & H_0 \\ N\left(P^r(k), M\sigma_0^2/2\right), & H_1 \end{cases} \tag{4}$$

$$X_t^i(k) : \begin{cases} N\left(0, M\sigma_0^2/2\right), & H_0 \\ N\left(P^i(k), M\sigma_0^2/2\right), & H_1 \end{cases} \tag{5}$$

where $P(k) = 0, 1, \cdots, M\text{-}1$, is the Fourier transform of the $s(n)$, $k = 0, 1, \cdots, M\text{-}1$, and the real part and imaginary part are $P^r(k)$ and $P^i(k)$, respectively. According to the statistical characteristics of $X_t^r(k)$ and $X_t^i(k)$, in the case of H_0,

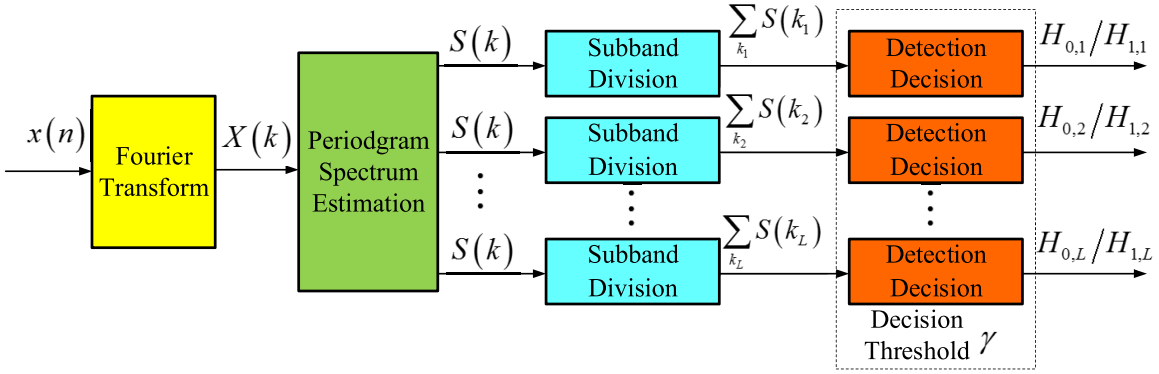

FIGURE 2. The block diagram of the spectrum sensing algorithm based on conventional spectral estimation.

$S_t(k)$ obeys a central chi-square distribution with degree of freedom be 2, and in the case of H_1, $S_t(k)$ obeys a non-central chi-square distribution with degree of freedom be 2, i.e,

$$\begin{cases} S_t(k) \sim \chi_2^2, & H_0 \\ S_t(k) \sim \chi_2^2(\zeta), & H_1 \end{cases} \tag{6}$$

where ζ is a non-central parameter, $\zeta = |P(k)|^2$, $E\left(\chi_2^2\right) = \sigma_0^2$, $D\left(\chi_2^2\right) = \sigma_0^4$, $E\left(\chi_2^2(\zeta)\right) = |P(k)|^2/M + \sigma_0^2$, $D\left(\chi_2^2(\zeta)\right) = \sigma_0^4 + 2\sigma_0^2|P(k)|^2/M$.

It can be seen from property b) of **Lemma 1** that Fourier transform data at different frequency points $X_t(k)$, $k = 0, 1, \cdots, M\text{-}1$, are independent of each other, and the periodogram estimation $S_t(k)$, $k = 0, 1, \cdots, M\text{-}1$ is a continuous function of $X_t(k)$ with finite discontinuities. So periodogram estimations $S_t(k)$, $k = 0, 1, \cdots, M\text{-}1$ at different frequencies are uncorrelated, which is derived from **Lemma 2**. Hence, we have

$$cov\left(S_t(p),\ S_t(q)\right) = 0 \quad p, q \in [0, M-1],\ p \neq q \tag{7}$$

Property c) of the **Lemma 1** also shows that Fourier transforms of different data frame at the same frequency point are independent of each other. The mean value and variance of the time averaged periodogram spectrum estimation, denoted by $S_{avg}(k)$, can be obtained by linear operation of the mean value and variance of $S_t(k)$, respectively. In the case of H_0, the mean value and variance of $S_{avg}(k)$ are $\mu_{avg,H_0} = E\left(\chi_2^2\right)$ and $\sigma^2_{avg,H_0} = D\left(\chi_2^2\right)/T$, respectively. In the case of H_1, the mean and value variance of $S_{avg}(k)$ are $\mu_{avg,H_1} = E\left(\chi_2^2(\zeta)\right)$ and $\sigma^2_{avg,H_1} = D\left(\chi_2^2(\zeta)\right)/T$, respectively.

III. THE BDNP ALGORITHM

The spectrum sensing algorithm based on conventional spectral estimation and the spectrum sensing algorithm based on bidirectional search of normalized spectrum both make use of the distinction of periodogram estimation under the case of H_0 and H_1 to determine the existence of the primary user signal. Since the BDNP algorithm originates from the CSE algorithm, it is necessary to briefly introduce the CSE based spectrum-sensing algorithm and its defect.

A. THE SPECTRUM SENSING ALGORITHM BASED ON CONVENTIONAL SPECTRAL ESTIMATION

The principle of the spectrum sensing algorithm based on conventional spectral estimation is shown in Fig 2. The algorithm first continuously takes M points of data from discrete sample $x(n)$, and performs discrete Fourier transform on the samples and the periodogram estimation to obtain $X(k)$, $k = 0, 1, \cdots, M\text{-}1$, and the power spectrum $S_{avg}(k)$, $k = 0, 1, \cdots, M\text{-}1$,respectively. And then the positive frequency portion of the power spectrum is divided into L frequency slots to calculate the power $S_{seg}(l)$, $l = 0, 1, \cdots, L\text{-}1$ in each frequency slot. Finally, it compares the frequency slot power with the decision threshold γ to determine whether there is a signal in the frequency slot: If frequency slot power exceeds the threshold γ, there is a signal in this frequency slot; Otherwise, there is no signal in the frequency slot. If there exists at least one frequency slot occupied among L frequency slots, it is determined that there is a signal in the entire frequency hopping bandwidth, i.e., the hypothesis H_1 is established. If no signal exists in L frequency slots, it is determined that there is no signal in the entire frequency band, i.e., the hypothesis H_0 is established.

If $L = M/2$, each frequency slot contains only one frequency point. The probability distribution of the frequency point is given by Eq.(1). Therefore, the false alarm probability P^l_{fa} and the correct detection probability of the frequency slot power P^l_d can be expressed as

$$P^l_{fa} = \Pr\left(S_{seg}(l) > \gamma \,|H_0\right) = \exp\left(-\frac{\gamma}{2\sigma_0^4}\right) \tag{8}$$

$$P^l_d = \Pr\left(S_{seg}(l) > \gamma \,|H_1\right) = Q_1\left(\frac{a}{\sigma}, \frac{\sqrt{\gamma}}{\sigma}\right) \tag{9}$$

where $l = 1, 2, \cdots, L$, $Q_1(\alpha, \beta)$ is the first order *MarcumQ* function, and $a = |P(l)|^2/M$, $\sigma = \sigma_0^4 + 2\sigma_0^2|P(l)|^2/M$.

If $L = M/2F$ and $F \geq 20$, each frequency slot contains a large number of frequency points, and the frequency slot power is the sum of the power of multiple frequency points. It can be known from the central limit theorem that the frequency slot power approximates the Gaussian distribution,

which means the false alarm probability P_{fa}^{l} and the correct detection probability P_{d}^{l} can be expressed as:

$$\begin{aligned} P_{fa}^{l} &= \Pr\left(S_{seg}\left(l\right) > \gamma \,|H_0\right) \\ &= 1/2 - 1/2\Phi\left(\frac{\gamma - \mu_{H_0}}{\sqrt{2}\sigma_{H_0}}\right) \end{aligned} \tag{10}$$

$$\begin{aligned} P_{d}^{l} &= \Pr\left(S_{seg}\left(l\right) > \gamma \,|H_1\right) \\ &= 1/2 - 1/2\Phi\left(\frac{\gamma - \mu_{H_1}}{\sqrt{2}\sigma_{H_1}}\right) \end{aligned} \tag{11}$$

where $\mu_{H_0} = \sum_F E\left(\chi_2^2\right)$, $\mu_{H_1} = \sum_F E\left(\chi_2^2\left(\zeta\right)\right)$, $\sigma_{H_0}^2 = \sum_F D\left(\chi_2^2\right)$, $\sigma_{H_1}^2 = \sum_F D\left(\chi_2^2\left(\zeta\right)\right)$.

Eqs.(8) and (10) shows that the false alarm probabilities of L frequency slots $P_{fa}^{l}, l = 1, 2, \cdots, L$ are the same, uniformly represented as $P_{fa}^{\prime}$. Then the false alarm probability of the CSE algorithm can be obtained by applying "OR" rule to all the $P_{fa}^{\prime}$ as follows:

$$P_{fa,CSE} = 1 - (1 - P_{fa}^{\prime})^{L}. \tag{12}$$

The CSE spectrum-sensing algorithm uses classical methods such as periodogram to calculate the power spectrum of received signals, and then divides the power spectrum into frequency slots with equal bandwidth to compare with the preset threshold to determine the occupancy status. This algorithm is simple to implement, but the threshold value needs to be determined according to the noise power as the frequency slot power is taken as test statistics. Once the noise power fluctuates, the decision threshold is difficult to determine. As a result, the spectrum sensing performance is sensitive to the noise uncertainty.

B. THE STEPS OF THE BDNP ALGORITHM

The BDNP algorithm uses the normalized power spectrum as the test statistic, and performs forward and backward searches in loops to find the occupied frequency slots within the frequency hopping bandwidth. In a search loop, the BDNP algorithm first performs a forward search to sense the frequency slots with larger instantaneous power. If the forward search fails, the algorithm performs a backward search to sense the occupied frequency slots which are missed to detect in forward decision. Fig.3 illustrates the algorithm steps, and the schematic diagram is shown in Fig.4.

1) Initialization. Set the number of initial loops i to be 1, the number of occupied segments perceived in the current loop m^i to be zero, the number of valid segments to detect in the current detection L^i to be L, and the loop-sensing decision results $R^i(l)$ to be 0, $l = 0, \cdots, L^i$-1. Then, the sampled sequence is divided into T frames, and the t-th frame is $x_t(n)$, $n = 0, 1, \cdots, M$-1, $t = 1, 2, \cdots, T$, where M is the number of samples per frame.

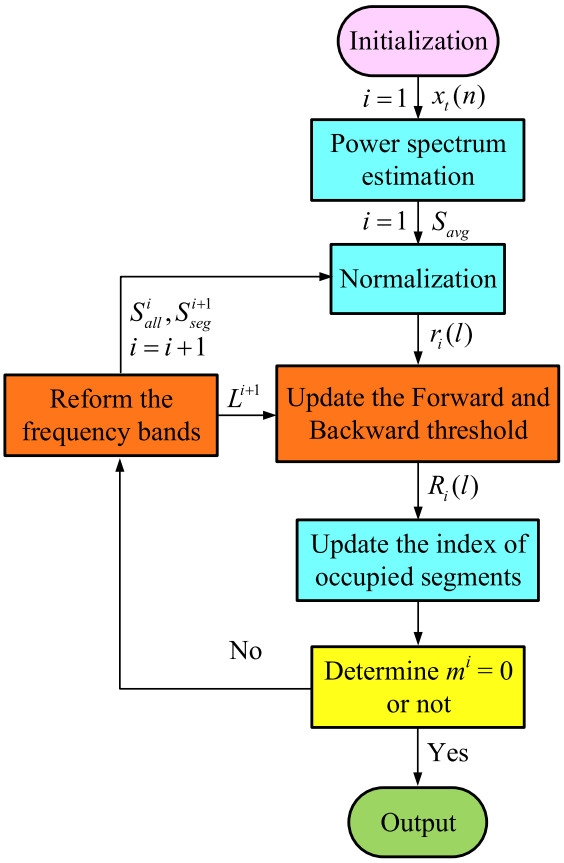

FIGURE 3. The flowchart of the BDNP algorithm.

2) Perform periodogram estimation of the power spectrum for each frame of data $x_t(n)$:

$$\begin{aligned} S_t\left(k\right) &= \frac{1}{M}\left|X_t\left(k\right)\right|^2 \\ &= \frac{1}{M}\left|\sum_{n=0}^{M-1} x_t\left(n\right) e^{-j2\pi kn/M}\right|^2, \quad 0 \le k \le M-1 \end{aligned} \tag{13}$$

The periodogram estimation of T frames of data is time averaged to obtain a flatter power spectrum. Since $x_t(n)$ is a real stationary signal, the positive and negative frequency power spectrum of each frame of data are symmetric, and $M/2$ points are required to completely represent its power spectrum. Calculate the average of the power spectrum of consecutive T frames to obtain the following:

$$S_{avg}\left(k\right) = \frac{1}{T}\sum_{t=1}^{T} S_t\left(k\right), \quad k = 1, \cdots, M/2 \tag{14}$$

3) Define the sum power of all spectral lines of the average of the power spectral density $S_{avg}(k)$ obtained in step 2) as S_{all}, and that of spectral lines in one segment is defined as S_{seg}, that is:

$$S_{all} = \sum_{k} S_{avg}\left(k\right), \quad k \in [1, M/2] \tag{15}$$

$$S_{seg} = \sum_{k} S_{avg}\left(k\right), \quad k \in \left[\frac{M^{\prime}l}{2} + 1, \frac{M^{\prime}\left(l+1\right)}{2}\right] \tag{16}$$

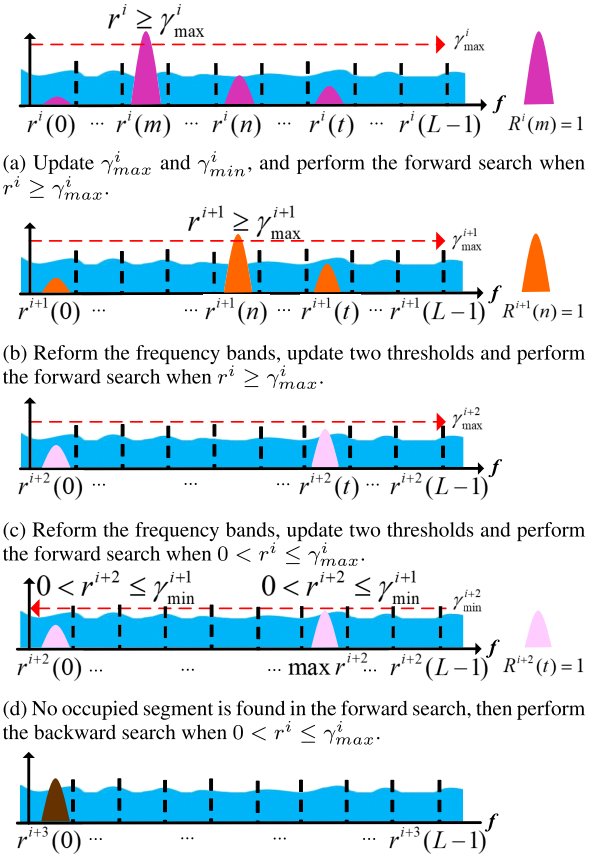

(a) Update γ^i_{max} and γ^i_{min}, and perform the forward search when $r^i \geq \gamma^i_{max}$.

(b) Reform the frequency bands, update two thresholds and perform the forward search when $r^i \geq \gamma^i_{max}$.

(c) Reform the frequency bands, update two thresholds and perform the forward search when $0 < r^i \leq \gamma^i_{max}$.

(d) No occupied segment is found in the forward search, then perform the backward search when $0 < r^i \leq \gamma^i_{max}$.

(e) Perform loops until no occupied segment is found in a single loop.

FIGURE 4. The schematic diagram of the BDNP algorithm.

where M' is the number of spectral lines in one segment.

4) Define the ratio of S_{seg} and S_{all} as the normalized power spectrum which is used as the test statistic of this algorithm:

$$r(l) = \frac{S_{seg}}{S_{all}}, \quad l = 0, 1, \cdots, L^i - 1 \tag{17}$$

5) Update the upper threshold γ^i_{max} and the lower threshold γ^i_{min} of the current loop. First, perform the forward search and compare the normalized power spectrum $r^i(l)$, $l = 0, 1, \cdots, L^i$ - 1, with the preset threshold γ^i_{max}. For $r^i(l) \geq \gamma^i_{max}$, then set the elements in the decision array $R^i(l)$ to 1, otherwise, set them to 0, which is called a forward single decision. Second, calculate the support set $\Lambda^i = supp\left(R^i\right)$ of $R^i(l)$ which is a set of non-zero element index numbers in $R^i(l)$, corresponding to the occupied segments in the current sensing loop. Therefore, the occupancy status of segments within the entire hopping bandwidth is given by $\Lambda^i_{all} = \Lambda^{i-1}_{all} \cup \Lambda^i$, where $\Lambda^0_{all} = 0$. Finally, calculate the potential of the support set of $R^i(l)$ which is $m^i = \left\|\Lambda^i\right\|_0$, corresponding to the number of segments occupied in the current sensing loop. For $m^i \neq 0$, then jump to step 7), and for $m^i \neq 0$, go to step 6).

6) Enter the backward search, and compare the normalized power spectrum $r^i(l)$, $l = 0, 1, \cdots, L^i$-1, with the preset threshold γ^i_{min}, which is called a backward single decision. For $0 < r^i(l) \leq \gamma^i_{min}$, find out the the index of the maximum of $r^i(l)$, represented as l_{max}, and set $R^i(l_{max})$ to 1 and $R^i(l) = 0$, $l \neq l_{max}$. If $0 < r^i(l) \leq \gamma^i_{min}$ does not hold, then set $R^i(l)$ to zero. Similar to step 5), calculate the support set $\Lambda^i of\ R^i$ and the potential m^i of the support set to update the occupancy status of Λ^i_{all} segments within the entire frequency hopping bandwidth. For $m^i \neq 0$, jump to step 7). For $m^i \neq 0$, then jump to step 8).

7) Update $S^{i+1}_{seg}(l)$, $S^{i=1}_{all}$ and l^{i+1} according to the following rules, and jump to step 4) to continue.

$$S^{i+1}_{seg}\left(\Lambda^i\right) = 0, \quad S^{i+1}_{all} = \sum_{l=0}^{L-1} S^{i+1}_{seg}, \ L^{i+1} = L^i - m^i \tag{18}$$

8) Output the set Λ^i_{all}. The elements in the set Λ^i_{all} correspond to the occupied frequency slots and the elements in its complementary set λ correspond to the segments of spectrum holes.

The full BDNP algorithm is summarized in Algorithm 1.

IV. PERFORMANCE ANALYSIS

A. FALSE ALARM PROBABILITY AND DECISION THRESHOLD OF THE BDNP ALGORITHM SEARCH LOOP

Under the hypothesis of H_0, the mean value and variance of the average of power spectrum $S_{avg,H_0}(k), k = 1, \cdots, M/2$ are $\mu_{avg,H_0} = \sigma_0^2$, $\sigma^2_{avg,H_0} = \sigma_0^4/T$, respectively. Any two of the spectrum lines in $S_{avg,H_0}(k)$ are uncorrelated known from Eq.(7). Then we construct random variables $X = S_{seg}$ and $Y = S_{all} - S_{seg}$. According to the central limit theorem, when the number of spectral lines are large enough (the number of general samples is greater than 20), the random variables X, Y approximate the Gaussian distribution, and the mean value and variance are respectively given by $\mu_{X,H_0} = M'\mu_{avg,H_0}/2$, $\sigma^2_{X,H_0} = M'\sigma^2_{avg,H_0}/2$ and $\mu_{Y,H_0} = \left(M - M'\right)\mu_{avg,H_0}/2$, $\sigma^2_{Y,H_0} = \left(M - M'\right)\sigma^2_{avg,H_0}/2$. The BDNP algorithm may contains a forward search and a backward search in a search loop. The false alarm probability of a single forward decision $P_{fa,F}$ and a single backward single decision $P_{fa,R}$ can be expressed as

$$\begin{aligned} P_{fa,F} &= P\left(\frac{X}{X+Y} > \gamma_{max} \,|H_0\right) \\ &= \frac{1}{2} + \frac{1}{2}\phi\left(\frac{\mu_{X,H_0}(1/\gamma_{max} - 1) - \mu_{Y,H_0}}{\sqrt{2}\sigma_{Y,H_0}\sqrt{(\sigma_{X,H_0}(1/\gamma_{max} - 1)/\sigma_{Y,H_0})^2 + 1}}\right) \end{aligned} \tag{19}$$

$$\begin{aligned} P_{fa,R} &= P\left(\frac{X}{X+Y} < \gamma_{min} \,|H_0\right) = \frac{1}{2} \\ &\quad - \frac{1}{2}\phi\left(\frac{\mu_{X,H_0}(1/\gamma_{min} - 1) - \mu_{Y,H_0}}{\sqrt{2}\sigma_{Y,H_0}\sqrt{(\sigma_{X,H_0}(1/\gamma_{min} - 1)/\sigma_{Y,H_0})^2 + 1}}\right) \end{aligned} \tag{20}$$

Algorithm 1 BDNP Algorithm

Input: the number of frames used T, the number of samples in each frame M, the number of valid segments to detect in the first detection L, and the number of spectral lines in one segment M'.

1: The t-th frame of the sampled sequence is $x_t(n), n = 0, 1, \cdots, M-1, t = 1, 2, \cdots, T$.
2: Initialize $i = 1$, and set $m^i = 0, L^i = L, \Lambda^i_{all} = 0, R^i(l) = 0, l = 0, 1, \cdots, L^1 - 1$.
3: Calculate:
$S_t(k) = |X_t(k)|^2/M = |\sum_{n=0}^{M-1} x_t(n)e^{-j2\pi kn}/M|^2/M$;
$S_{avg}(k) = \sum_{t=1}^{T} S_t(k)/T$;
$S_{all} = \sum_k S_{avg}(k), k \in [1, M/2]$;
$S_{seg} = \sum_k S_{avg}(k), k \in \left[M'l/2 + 1, M'(l+1)/2\right]$.
4: **repeat**
5: Calculate $r^i(l) = S_{seg}/S_{all}$, and update the upper threshold γ^i_{max} and the lower threshold γ^i_{min} of the current loop.[1]
6: Perform **The Forward Search**:
For $r^i(l) \geq \gamma^i_{max}$, set $R^i(l) = 1$; Otherwise, set $R^i(l) = 0$.
Calculate $\Lambda^i = supp(R^i)$, and set $\Lambda^i_{all} = \Lambda^{i-1}_{all} \cup \Lambda^i$, $m^i = \|\Lambda^i\|_0$.
For $m^i \neq 0$, update $S^{i+1}_{seg}(\Lambda^i) = 0$, $S^{i+1}_{all} = \sum_{l=0}^{L-1} S^{i+1}_{seg}$, $L^{i+1} = L^i - m^i$; Otherwise, jump to **step 7**.
7: Perform **The Backward Search**:
For $0 < r^i(l) \leq \gamma^i_{min}$, set $l_{max} = \arg\min_l r^i(l)$, $R^i(l_{max}) = 1, R^i(l) = 0, l \neq l_{max}$;Otherwise, set $R^i(l) = 0$.
Calculate $\Lambda^i = supp(R^i)$, and set $\Lambda^i_{all} = \Lambda^{i-1}_{all} \cup \Lambda^i$, $m^i = \|\Lambda^i\|_0$.
For $m^i \neq 0$, update $S^{i+1}_{seg}(\Lambda^i) = 0$, $S^{i+1}_{all} = \sum_{l=0}^{L-1} S^{i+1}_{seg}$, $L^{i+1} = L^i - m^i$; Otherwise, Output the index of the occupied segments Λ^i_{all}.
8: **until** No occupied segment is found in the forward and backward search of a single loop.

According to the Neyman-Pearson criterion, the forward search threshold γ_{max} and the backward search threshold γ_{min} can be respectively determined from the preset target false alarm probabilities $P_{fa,F}$ and $P_{fa,R}$. By substituting $P_{fa,F}$ and $P_{fa,R}$ into Eq.(19) and (20), respectively, and setting $M = LM'$, we can obtain closed expressions of γ_{max} and γ_{min} at the bottom of this page, where $\phi(\cdot)$ is the error function and $\phi^{-1}(\cdot)$ is its inverse function. It can be known from Eq.(21) and (22), as shown at the bottom of this page, that the threshold γ_{max} and γ_{min} of the BDNP sensing algorithm are related to the frame length M, the number of frames T, the number of segments L, and the false alarm probability P_{fa}, but independent of the noise variance σ_0^2. Therefore, the threshold of the BDNP sensing algorithm is determined independently of the noise level and not affected by the noise uncertainty. BDNP spectrum sensing consists of multiple forward and backward search loops, while the frame length M, the number of frames T, and segment false alarm probability P_{fa} used in each loop are constant. Only the number of participating segments is changed according to Eq.(18).

[1]Calculate two thresholds by using Eqs.(21) and (22).

B. FALSE ALARM PROBABILITY OF THE BDNP ALGORITHM

If given the target false alarm probability $P_{fa,F}$ and $P_{fa,R}$ and the number of segments L, the false alarm probability of a single search loop can be expressed as:

$$P_{fa,CYC} = 1 - (1 - P_{fa,F})^L + (1 - P_{fa,F})^L \left(\sum_{k=1}^{L} (1 - P_{fa,R})^{k-1} P_{fa,R} \right) \quad (23)$$

Since the BDNP algorithm is an iterative algorithm, and the stop condition of iterations depends on whether the potential of the support set of the decision result array R^i gets zero, rather than fixedly stopping iteration. Therefore, the false alarm probability of the BDNP algorithm cannot be accurately determined. However, when running the BDNP algorithm, the search loop of the L-segment is executed at least once, and the search loop of different number of segments is executed at most L times. The condition for proceeding the next search loop is that there comes false alarm in the previous search loop, so the upper and lower bounds of the algorithm false alarm probability $P_{fa,BDNP}$ can be expressed as:

$$P_{fa,CYC} \leq P_{fa,BDNP} \leq \sum_{j=1}^{L} \prod_{i=1}^{j} P^i_{fa,CYC} \quad (24)$$

where $P_{fa,CYC}$ is the false alarm probability of a single search loop in the case of L-segments. The false alarm probability $P^i_{fa,CYC}$ of the i-th search loop can be calculated by the Eq.(23), where L^i is the number of valid segments involved in the i-th loop detection. Within the frequency hopping bandwidth, if it is given that the signal-to-noise ratios of the

$$\gamma_{max} = \frac{1}{L} + \frac{2\sqrt{TM(L-1)[\phi^{-1}(1-2P_{fa,F})]^2 - 4(L-1)[\phi^{-1}(1-2P_{fa,F})]^4}}{TML - 4L[\phi^{-1}(1-2P_{fa,F})]^2} \quad (21)$$

$$\gamma_{min} = \frac{1}{L} - \frac{2\sqrt{TM(L-1)[\phi^{-1}(1-2P_{fa,R})]^2 - 4(L-1)[\phi^{-1}(1-2P_{fa,R})]^4}}{TML - 4L[\phi^{-1}(1-2P_{fa,R})]^2} \quad (22)$$

primary user signals differs large, the configuration can be set as $P_{fa,F} > P_{fa,R}$ to ensure a high correct detection probability. Otherwise, the configuration can be set as $P_{fa,F} < P_{fa,R}$, to further reduce the probability of missed detection. This paper focuses on blind spectrum sensing performance of the BDNP algorithm in CR systems, without loss of generality, let $P_{fa,F} = P_{fa,R} = P_{fa}$.

C. DETECTION PROBABILITY OF THE BDNP ALGORITHM

Under the hypothesis of H_1, the mean value of the average of power spectrum $S_{avg,H_1}(k)$ is $\mu_{avg,H_1} = |P(k)|^2/M + \sigma_0^2$, and the variance is $\sigma^2_{avg,H_1} = \sigma_0^4/T + 2\sigma_0^2|P(k)|^2/TM$. We construct random variables $X = S_{seg}$ and $Y = S_{all}$. The power spectrum at different frequency points in $S_{avg,H_1}(k)$ are uncorrelated, which is known by Eq.(7). According to the central limit theorem, X and Y can be approximated as random variables obeying the Gaussian distribution, and the mean value and variance are respectively

$$\begin{aligned}\mu_{X,H_1} &= \sum_k \mu_{avg,H_1}, \quad \sigma^2_{X,H_1} \\ &= \sum_k \sigma^2_{avg,H_1}, \quad k \in \left[\frac{M'l}{2}+1, \frac{M'(l+1)}{2}\right] \\ \mu_{Y,H_1} &= \sum_k \mu_{avg,H_1}, \quad \sigma^2_{Y,H_1} \\ &= \sum_k \sigma^2_{avg,H_1}, \quad k \in \left[1, \frac{M}{2}\right]\end{aligned} \tag{25}$$

Similar to the calculation of the false alarm probability, the BDNP algorithm consists of a forward search and a backward search in one search loop. The detection probability of a forward single decision $P_{d,l,F}$ and a backward single decision $P_{d,l,R}$ can be expressed as

$$\begin{aligned}&P_{d,l,F} \\ &= P\left(\frac{X}{Y} > \gamma_{max}\,|H_1\right) = \frac{1}{2} \\ &\quad + \frac{1}{2}\phi\left(\frac{\mu_{X,H_1}/\gamma_{max} - \mu_{Y,H_1}}{\sqrt{2(\sigma_{X,H_1}(1/\gamma_{max}-1))^2 + 2(\sigma_{Y,H_1}-\sigma_{X,H_1})^2}}\right)\end{aligned} \tag{26}$$

$$\begin{aligned}&P_{d,l,R} \\ &= P\left(\frac{X}{Y} < \gamma_{min}\,|H_1\right) = \frac{1}{2} \\ &\quad - \frac{1}{2}\phi\left(\frac{\mu_{X,H_1}/\gamma_{min} - \mu_{Y,H_1}}{\sqrt{2(\sigma_{X,H_1}(1/\gamma_{min}-1))^2 + 2(\sigma_{Y,H_1}-\sigma_{X,H_1})^2}}\right)\end{aligned} \tag{27}$$

Given the forward and backward threshold γ_{max}, γ_{min} and the number of segments L, the detection probability of a single search loop can be expressed as:

$$\begin{aligned}&P_{d,CYC} \\ &= 1 - \prod_{l=0}^{L-1}(1-P_{d,l,F}) \\ &\quad + \left(\prod_{l=0}^{L-1}(1-P_{d,l,F})\right)\sum_{k=1}^{L}\left(\left(\prod_{l=0}^{k-1}(1-P_{d,l,R})\right)P_{d,k,R}\right)\end{aligned} \tag{28}$$

Since the BDNP algorithm mainly focuses on the wideband multi-signal spectrum sensing, we simulate the detection probability of the BDNP algorithm with one single signal to prove the rationality of this algorithm and we simulate the multi-signal sensing performance to prove the BDNP algorithm can adapt to the wideband multi-signal spectrum sensing in the next section.

For the discussion in the next section, the analysis of the detection probability of fading channels is given here. Specially, the channel coefficient $h(t)$ is a complex Gauss random variable under the fading channels. Under the Rayleigh channel, the mean value of the average of power spectrum $S_{avg,H_1}(k)$ is $\mu_{avg,H_1} = G(k)|P(k)|^2/M + \sigma_0^2$, and the variance is $\sigma^2_{avg,H_1} = (G(k) + M\sigma_0^2)^2/TM^2$, where $G(k) = \sum_{m=0}^{M/p-1}\left|\sum_{n=0}^{p-1} s(pm+n)exp(-j\frac{2\pi}{M}kn)\right|^2$. Under the Rice channel, the mean value of the average of power spectrum $S_{avg,H_1}(k)$ is $\mu_{avg,H_1} = (\kappa/(\kappa+1) + G(k)/(\kappa+1))|P(k)|^2/M + \sigma_0^2$, and the variance is $\sigma^2_{avg,H_1} = (G(k)/(\kappa+1) + M\sigma_0^2)^2/TM^2 + 2\kappa|P(k)|^2(G(k)/(\kappa+1) + M\sigma_0^2)/TM^2(\kappa+1)$, where κ is the Rice factor. Similar to the detection probability of the AWGN channels, we can obtain the detection probability of a single search loop under the fading channels using the Eqs.(26)-(28).

D. COMPUTATIONAL COMPLEXITY OF THE BDNP ALGORITHM

It can be seen from the steps of the BDNP algorithm that its computational complexity is mainly determined by that of the periodogram spectral estimation. The periodogram spectral estimation first performs the discrete Fourier transform on data, and then calculates the square of the resulting modulus to obtain the power spectrum. In the BDNP algorithm, M-point Fourier transform is performed for each frame, thus the computational complexity of this part is $O(M^2)$. Normalizations and threshold decisions are performed when entering the bidirectional searches, and the number of divisions in the normalization of one loop decreases with occupied segments continuously found after each bidirectional search. Since the number of total bidirectional search loop is not more than the number of signals existing in the frequency bands (except the situation of false alarm), the computational complexity of this part is very low, which is calculated to be $O(L)$ if there are L valid segments to detect. The superiority of the BDNP algorithm is that the power spectrum estimation needs to be performed only one time for the whole algorithm.

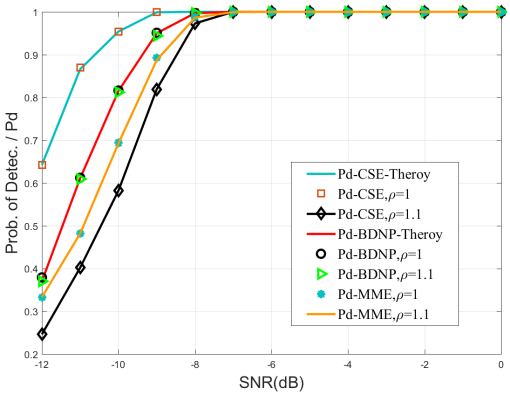

FIGURE 5. The comparison of the correct detection probability of the CSE algorithm, MME detection and the BDNP algorithm in a single loop.

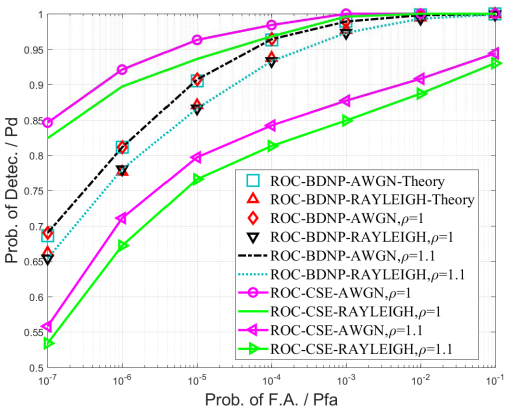

FIGURE 6. The comparison of the ROC curves of the CSE algorithm and the BDNP algorithm in a single loop under the AWGN and Rayleigh channels.

When occupied segments are taken out of the frequency bands, this algorithm just updates coefficients to recalculate the forward and backward threshold and performs next search loop. In summary, the computational complexity of the BDNP algorithm is low, which makes it possible to adapt to real-time wideband multi-signal spectrum sensing.

V. ALGORITHM SIMULATIONS AND RESULT ANALYSIS

A. THE PERFORMANCE OF ROBUSTNESS TO NOISE UNCERTAINTY

According to the system model described above, the Monte Carlo method is used to simulate the performance of the BDNP algorithm in a single loop, which is compared with that of the CSE spectrum-sensing algorithm. We assume that under the AWGN, Rayleigh and Rice channels, the signal bandwidth and the carrier frequency of the digital modulated signal transmitted by primary users are respectively $1.28MHz$ and $5.12MHz$, and secondary users sample the received signal with a sampling rate of 12.8 *Msps*. We characterize the noise uncertainty in spectrum sensing that when it exists, the noise variance obeys a uniform distribution with a range of $\left(\sigma_0^2/\rho, \rho\sigma_0^2\right)$, where $\rho > 1$, and if there is no noise uncertainty, $\rho = 1$. When analyzing the single-loop sensing performance of the CSE spectrum-sensing algorithm and the BDNP algorithm, the principle of constant false alarm probability is adopted, and the false alarm probability is preset as 0.01.

Fig.5 compares the correct detection probability of the CSE algorithm, maximum-minimum eigenvalue (MME) detection [36] and the BDNP algorithm in a single loop with the normalized SNR varying from $-12dB$ to $0dB$ in the case of $\rho = 1$ and $\rho = 1.1$, respectively. In this simulation, the number of samples used by the CSE algorithm, MME detection and the BDNP algorithm is 4000, the number of frames of the BDNP algorithm T is set to 1, the length of each frame M is set as 4000, and the number of segments L is set to be 4. In the case of $\rho = 1$, according to the principle of constant false alarm probability, the decision threshold of a single loop of the BDNP algorithm can be

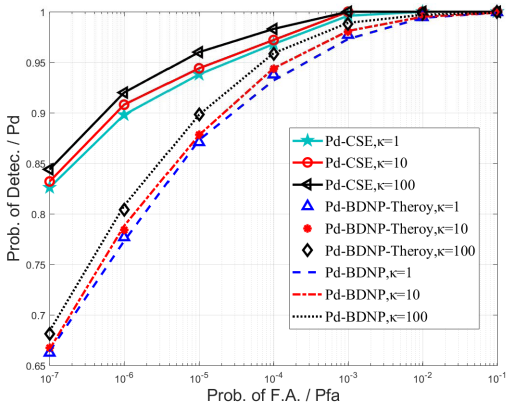

FIGURE 7. The comparison of the ROC curves of the CSE algorithm and the BDNP algorithm in a single loop under the Rice channel.

obtained by Eqs.(21)-(23), and the decision threshold of the CSE algorithm can be obtained by Eqs.(8) and (12). In the case of $\rho = 1.1$, the decision threshold of the CSE algorithm needs to be properly adjusted to ensure that the actual false alarm probability is equal to the preset value, on the contrary, the decision threshold of the BDNP algorithm is independent of the noise variance, so there is no need for adjustments. It can be seen from Fig.5 that when there is no noise uncertainty, the simulation curve and the theoretical value curve of both the CSE algorithm and the BDNP algorithm match well, and the CSE algorithm outperforms the BDNP algorithm and MME detection. At $\rho = 1.1$, the detection performance of the BDNP algorithm becomes significantly better than that of the CSE algorithm. Although MME detection method can also overcome noise uncertainty, the performance of BDNP algorithm is superior to that of the MME method, which is very difficult (mathematically intractable) to obtain a precisely decision threshold.

Fig.6 shows the receiver operating characteristic curves (ROC) of the CSE and BDNP algorithm for a fixed normalized SNR of $-7dB$ when $\rho = 1$ and $\rho = 1.1$ under the AWGN channel and the Rayleigh channel. In this simulation, the sample length used by the two algorithms are consistent

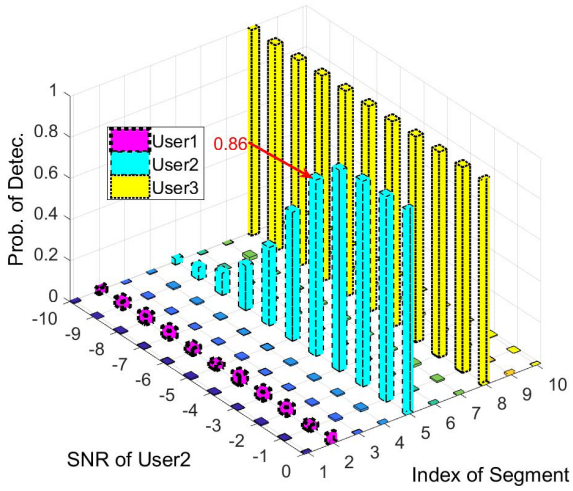

(a) The CSE algorithm, three primary users, $\rho = 1$.

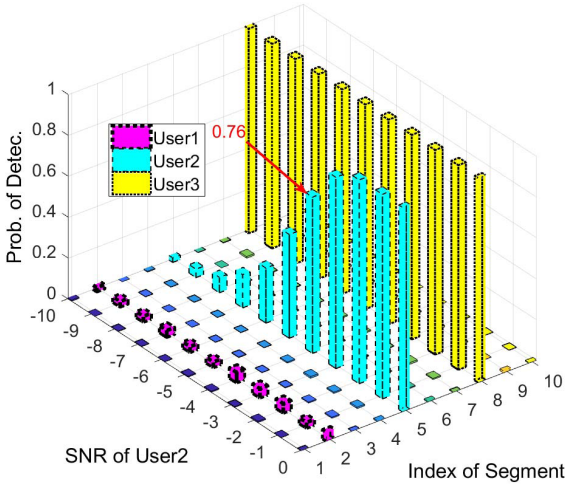

(b) The BDNP algorithm, three primary users, $\rho = 1$.

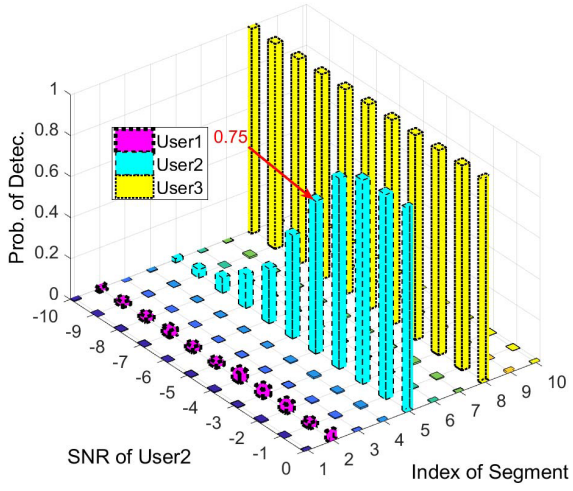

(c) The BDNP algorithm, three primary users, $\rho = 1.1$.

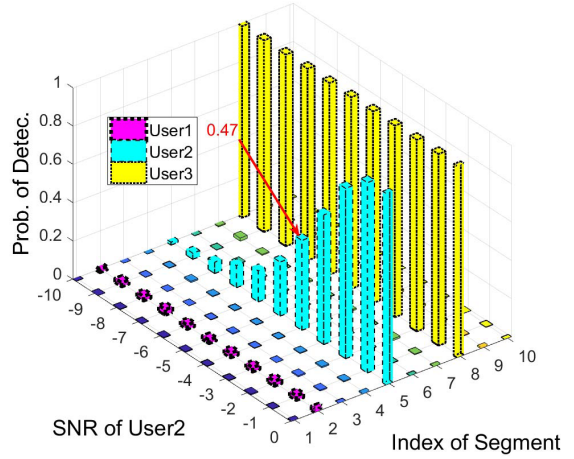

(d) The CSE algorithm, three primary users, $\rho = 1.1$.

FIGURE 8. **Multi-signal sensing performance of the BDNP algorithm and the CSE algorithm.**

with Fig.5. When $\rho = 1$, the simulation results of the BDNP algorithms are consistent with the theoretical value, and the ROC curves can be directly derived from the theoretical value of the algorithm. When $\rho = 1.05$, the ROC curves of the two algorithms are obtained by simulation, and the decision threshold of the CSE algorithm needs to be properly adjusted to ensure the accuracy of the false alarm probability. It can be seen from Fig.6 that there is a large deviation between two ROC curves of the CSE algorithm under different values of ρ, which is valid under the AWGN channel and the Rayleigh channel. Moreover, the simulation curve and the theoretical curve of the BDNP algorithm under the same channel are substantially coincident. In addition, it is known from Fig.5 and Fig.6 that the CSE algorithm is sensitive to the noise uncertainty, and the BDNP algorithm is robust to noise uncertainty. This is because the threshold of the CSE algorithm is determined by the noise variance, while that of the BDNP algorithm is independent of the noise variance.

Fig.7 shows the ROC curves of the CSE and BDNP algorithm for a fixed normalized SNR of $-7dB$ when the Rice factor $\kappa = 0.1$, 1 and 10 under the Rice channel. In this simulation, the sample length used by the two algorithms are consistent with Fig.5. It is known from Fig.6 and Fig.7 that the performance of the CSE and BDNP algorithm under the Rayleigh channel is slightly worse than that under the AWGN channel model. While the performance under the Rice channel is between the Rayleigh channel and the AWGN channel. Specifically, the smaller κ is, the closer the performance of the two algorithms is to that under the Rayleigh channel. The larger κ is, the closer the performance of the two algorithms is to that under the AWGN channel. The simulation values are basically consistent with the theoretical values.

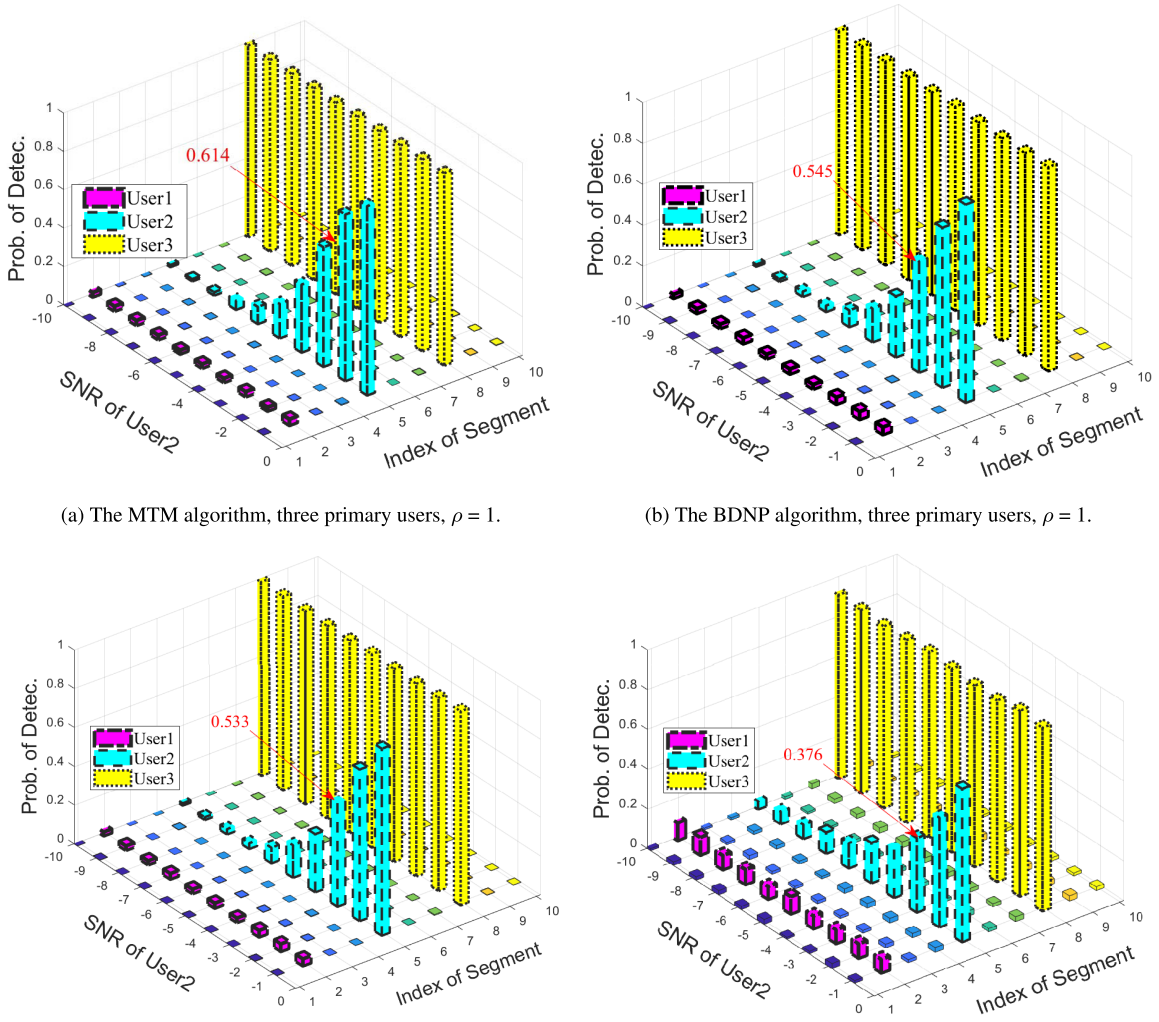

(a) The MTM algorithm, three primary users, $\rho = 1$.

(b) The BDNP algorithm, three primary users, $\rho = 1$.

(c) The BDNP algorithm, three primary users, $\rho = 1.1$.

(d) The MTM algorithm, three primary users, $\rho = 1.1$.

FIGURE 9. **Multi-signal sensing performance of the BDNP algorithm and the MTM algorithm.**

B. MULTI-SIGNAL SENSING PERFORMANCE OF THE BDNP ALGORITHM

Fig.8 simulates the spectrum sensing performance of the CSE algorithm and the BDNP algorithm when there are multiple primary user signals in the monitored frequency band. Assume that under the AWGN channel, all three primary users transmit digital modulated signals with a symbol rate of $0.5MBaud$. The carrier frequency of primary user one is $1.5MHz$, and the normalized signal-to-noise ratio stays unchanged as $-8dB$. The carrier frequency of primary user two is $4.5MHz$,and the normalized signal-to-noise ratio varies within the range of $-6dB$ $-2dB$. The carrier frequency of primary user three is $7.5MHz$, and the normalized signal-to-noise ratio stays as $0dB$. Secondary users sample the received signal at a sampling rate of $20MSPS$, and the definition of the noise uncertainty and the parameter setting of the sensing algorithm are as described above. It can be seen from Fig.8(a)-(d) that when there are three primary users in the monitored frequency band, the CSE algorithm has superior multi-signal spectrum sensing performance if there is no noise uncertainty, but will be seriously affected by noise uncertainty. The BDNP algorithm shows good performance in multi-signal spectrum sensing, and is confined to the noise uncertainty. This is because the decision threshold of each single-loop sensing of the BDNP algorithm is independent of the noise variance.

For further analysis of the multi-signal sensing performance of the BDNP algorithm, Fig.9 simulates the multi-signal spectrum sensing performance of the algorithm based on multi-taper method (MTM) [37] and the BDNP algorithm. Signal characteristic parameters, definition of the noise uncertainty and the parameter configuration of sensing algorithms are shown in Fig.8. Since the MTM algorithm uses multiple orthogonal window functions to estimate the power

spectrum of the signal sample sequence, for fair comparison, the sample length used in the MTM algorithm and the BDNP algorithm are both 4000, and the original samples are copied 5 times to form a sample sequence to be processed with a length of 20000. Moreover, the number of frames of the BDNP algorithm T is set as 5, the length of each frame M is set as 4000, the number of segments L is set as 10, the number of MTM algorithm windows is set as 5, and the data length per window is set as 4000.

It can be seen from Fig.9 that the spectrum sensing performance of the MTM algorithm is influenced by the noise uncertainty, which is similar to the CSE spectrum sensing algorithm and seriously restricts the applications of the MTM algorithm in low SNR occasions. By contrast, the BDNP algorithm has a good multi-signal spectrum sensing performance and the simulation results are consistent with theoretical analysis, because this algorithm is not sensitive to the noise uncertainty. As a result, in the presence of noise uncertainty, the multi-signal sensing performance of the BDNP algorithm is significantly better than the MTM algorithm. It is worth noting that there is a performance degradation of the BDNP algorithm in Fig. 9 compared to that of the result in Fig. 8, which is caused by the decrease in the number of samples. It can be concluded from Fig.8 and Fig.9 that compared to the spectrum-estimation-based sensing algorithms, no matter they are based on conventional spectral estimation or multi-window spectral estimation, the BDNP algorithm presents more stable and reliable sensing performance in the situation where the noise variance changes dynamically, and has certain advantages in sensing performance.

VI. CONCLUSION

In this paper, we proposed a spectrum-sensing algorithm based on bidirectional decision of normalized spectrum (BDNP) for the requirements of wideband, multiple frequency slots and real-time sensing in CR systems. This algorithm utilize bidirectional search and decision thresholds obtained by using Neyman-Pearson criterion, which can quickly and accurately monitor the frequency slots in the hopping bandwidth with a very low computational complexity, and makes this algorithm independent of the noise variance. The simulation results show that the BDNP algorithm can effectively overcome the influence of noise uncertainty on spectrum sensing performance, and achieve a high detection probability in a dynamic range of signal-to-noise ratio to complete the in-band multi-signal sensing. Therefore, the BDNP sensing algorithm can be widely applied to CR systems without interference to the primary users in complicated electromagnetic environments.

REFERENCES

[1] *Visual Networking Index: Forecast and Methodology 2016–2021*, Cisco, San Jose, CA, USA, 2017.
[2] Y. Chen and H. S. Oh, "A survey of measurement-based spectrum occupancy modeling for cognitive radios," *IEEE Commun. Surveys Tuts.*, vol. 18, no. 1, pp. 848–859, 1st Quart., 2016.
[3] V. Dhivya, P. Kalaiyarasi, and G. I. Shamini, "Survey on spectrum occupancy by using different techniques," in *Proc. Int. Conf. Comput. Power Energy Inf. Commun. (ICCPEIC)*, Melmaruvathur, India, 2017, pp. 316–320.
[4] S. Haykin and P. Setoodeh, "Cognitive radio networks: The spectrum supply chain paradigm," *IEEE Trans. Cogn. Commun. Netw.*, vol. 1, no. 1, pp. 3–28, Mar. 2015.
[5] D. Wang, B. Song, D. Chen, and X. Du, "Intelligent cognitive radio in 5G: AI-based hierarchical cognitive cellular networks," *IEEE Wireless Commun.*, vol. 26, no. 3, pp. 54–61, Jun. 2019.
[6] Z. Yao, W. Cheng, and H. Zhang, "Full-duplex assisted LTE-U/Wifi coexisting networks in unlicensed spectrum," *IEEE Access*, vol. 6, pp. 40085–40095, 2018.
[7] T. A. Atif, A. M. Baswade, B. R. Tamma, and A. A. Franklin, "A complete solution to LTE-U and WiFi hidden terminal problem," *IEEE Trans. Cogn. Commun. Netw.*, to be published.
[8] M. Rahmanil, "Frequency hopping in cognitive radio networks: A survey," in *Proc. IEEE Int. Conf. Wireless Space Extreme Environ. (WiSEE)*, Orlando, FL, USA, 2015, pp. 1–6.
[9] Z. Li, L. Guan, C. Li, and A. Radwan, "A secure intelligent spectrum control strategy for future THz mobile heterogeneous networks," *IEEE Commun. Mag.*, vol. 56, no. 6, pp. 116–123, Jun. 2018.
[10] H. Chen, M. Zhou, L. Xie, K. Wang, and J. Li, "Joint spectrum sensing and resource allocation scheme in cognitive radio networks with spectrum sensing data falsification attack," *IEEE Trans. Veh. Technol.*, vol. 65, no. 11, pp. 9181–9191, Nov. 2016.
[11] Q. Wu, G. Ding, J. Wang, and Y. D. Yao, "Spatial-temporal opportunity detection for spectrum-heterogeneous cognitive radio networks: Two-dimensional sensing," *IEEE Trans. Wireless Commun.*, vol. 12, no. 2, pp. 516–526, Feb. 2013.
[12] P. Qi, Z. Li, W. Cheng, J. Si, and Q. Wu, "Residual correlation matrix detection based blind sub-Nyquist spectrum sensing for cognitive radio networks," in *Proc. 9th Int. Conf. Wireless Commun. Signal Process. (WCSP)*, Nanjing, China, Oct. 2017, pp. 1–7.
[13] Y. Gao, Y. Chen, and Y. Ma, "Sparse-Bayesian-learning-based wideband spectrum sensing with simplified modulated wideband converter," *IEEE Access*, vol. 6, pp. 6058–6070, 2018.
[14] L. Zhang, G. Ding, Q. Wu, and Z. Han, "Spectrum sensing under spectrum misuse behaviors: A multi-hypothesis test perspective," *IEEE Trans. Inf. Forensics Security*, vol. 13, no. 4, pp. 993–1007, Apr. 2018.
[15] H. Sun, A. Nallanathan, C.-X. Wang, and Y. Chen, "Wideband spectrum sensing for cognitive radio networks: A survey," *IEEE Wireless Commun.*, vol. 20, no. 2, pp. 74–81, Apr. 2013.
[16] G. Ding, J. Wang, Q. Wu, L. Zhang, Y. Zou, Y.-D. Yao, and Y. Chen, "Robust spectrum sensing with crowd sensors," *IEEE Trans. Commun.*, vol. 62, no. 9, pp. 3129–3143, Sep. 2014.
[17] J. Zhao, Q. Liu, X. Wang, and S. Mao, "Scheduled sequential compressed spectrum sensing for wideband cognitive radios," *IEEE Trans. Mobile Comput.*, vol. 17, no. 4, pp. 913–926, Apr. 2018.
[18] J. Heydari and A. Tajer, "Quickest search and learning over correlated sequences: Theory and application," *IEEE Trans. Signal Process.*, vol. 67, no. 3, pp. 638–651, 1 Feb. 2019.
[19] J. Heydari and A. Tajer, "Quickest search and learning over multiple sequences," in *Proc. IEEE Int. Symp. Inf. Theory (ISIT)*, Aachen, Germany, Jun. 2017, pp. 1371–1375.
[20] H. Pradhan, S. S. Kalamkar, and A. Banerjee, "Sensing-throughput tradeoff in cognitive radio with random arrivals and departures of multiple primary users," *IEEE Commun. Lett.*, vol. 19, no. 3, pp. 415–418, Mar. 2015.
[21] A.-A. A. Boulogeorgos, N. D. Chatzidiamantis, and G. K. Karagiannidis, "Spectrum sensing with multiple primary users over fading channels," *IEEE Commun. Lett.*, vol. 20, no. 7, pp. 1457–1460, Jul. 2016.
[22] J. Mu, X. Jing, H. Huang, and N. Gao, "Subspace-based method for spectrum sensing with multiple users over fading channel," *IEEE Commun. Lett.*, vol. 22, no. 4, pp. 848–851, Apr. 2018.
[23] L. Chen, N. Zhao, Y. Chen, F. R. Yu, and G. Wei, "Over-the-air computation for cooperative wideband spectrum sensing and performance analysis," *IEEE Trans. Veh. Technol.*, vol. 67, no. 11, pp. 10603–10614, Nov. 2018.
[24] E. H. Salman, N. K. Noordin, S. J. Hashim, and F. Hashim, "A new cooperative spectrum sensing scheme based on discrete cosine transform," in *Proc. IEEE 3rd Int. Symp. Telecommun. Technol. (ISTT)*, Kuala Lumpur, Malaysia, Nov. 2016, pp. 108–111.

[25] N. Wang and Y. Gao, "Optimal threshold of Welch's Periodogram for sensing OFDM signals at low SNR levels," in *Proc. 19th Eur. Wireless Conf.*, Guildford, U.K., Apr. 2013, pp. 1–5.
[26] M. Bkassiny and S. K. Jayaweera, "Robust, non-Gaussian wideband spectrum sensing in cognitive radios," *IEEE Wireless Commun.*, vol. 13, no. 11, pp. 6410–6421, Nov. 2014.
[27] A. Taherpour, S. Gazor, and M. Nasiri-Kenari, "Wideband spectrum sensing in unknown white Gaussian noise," *IET Commun.*, vol. 2, no. 6, pp. 763–771, Jul. 2008.
[28] H. Qi and Y. Gao, "Two-dimensional compressive spectrum sensing in collaborative cognitive radio networks," in *Proc. IEEE Global Commun. Conf.*, Singapore, Dec. 2017, pp. 1–6.
[29] Y. Ma, Y. Gao, Y.-C. Liang, and S. Cui, "Efficient blind cooperative wideband spectrum sensing based on joint sparsity," in *Proc. IEEE Global Commun. Conf. (GLOBECOM)*, Washington, DC, USA, Dec. 2016, pp. 1–6.
[30] P. R. Muduli, A. K. Mandal, and A. Mukherjee, "An antinoise-folding algorithm for the recovery of biomedical signals from noisy measurements," *IEEE Trans. Instrum. Meas.*, vol. 66, no. 11, pp. 2909–2916, Nov. 2017.
[31] P. B. Gohain, S. Chaudhari, and V. Koivunen, "Cooperative energy detection with heterogeneous sensors under noise uncertainty: SNR wall and use of evidence theory," *IEEE Trans. Cogn. Commun. Netw.*, vol. 4, no. 3, pp. 473–485, Sep. 2018.
[32] P. J. Chung, J. F. Bohme, C. F. Mecklenbrauker, and A. O. Hero, "Detection of the number of signals using the benjamini-hochberg procedure," *IEEE Trans. Signal Process.*, vol. 55, no. 6, pp. 2497–2508, Jun. 2007.
[33] P. Zhang, "Energy detection using Savitzky-Golay smoothing method for spectrum sensing in cognitive radio," in *Proc. IEEE 8th Joint Int. Inf. Technol. Artif. Intell. Conf. (ITAIC)*, Chongqing, China, May 2019, pp. 1181–1185.
[34] A. V. Oppenheim, *Discrete-Time Signal Processing*, 3rd ed. Upper Saddle River, NJ, USA: Prentice-Hall, 2010.
[35] Y. L. Zhang, Q. Y. Zhang, and T. Melodia, "A frequency-domain entropy-based detector for robust spectrum sensing in cognitive radio networks," *IEEE Commun. Lett.*, vol. 14, no. 6, pp. 533–535, Jun. 2010.
[36] C. B. A. Wael, N. Armi, and B. P. A. Rohman, "Spectrum sensing for low SNR environment using maximum-minimum eigenvalue (MME) detection," in *Proc. Int. Seminar Intell. Technol. Appl. (ISITIA)*, Lombok, Indonesia, Jul. 2016, pp. 435–438.
[37] Q. T. Zhang, "Theoretical performance and thresholds of the multitaper method for spectrum sensing," *IEEE Trans. Veh. Technol.*, vol. 60, no. 5, pp. 2128–2138, Jun. 2011.

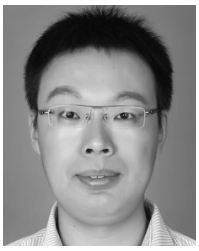

PEIHAN QI was born in Henan, China, in 1986. He received the B.S. degree in telecommunications engineering from Chang'an University, Xi'an, in 2006, and the M.S. degree in communication and information systems and the Ph.D. degree in military communication from Xidian University, in 2011 and 2014, respectively, where he has been an Associate Professor with the School of Telecommunications Engineering, since July 2018. He is interested in compressed sensing, spectrum sensing in cognitive radio networks, and high-speed digital signal processing.

YI DU was born in Shandong, China, in 1996. He received the B.S. degree in information engineering from Xidian University, in 2018, where he is currently pursuing the M.S. degree in telecommunication engineering. His research interests include machine learning, compressed sensing, and spectrum sensing in cognitive radio networks.

DANYANG WANG, photograph and biography not available at the time of publication.

ZAN LI was born in Shaanxi, China, in 1975. She received the B.S. degree in telecommunications engineering, and the M.S. and Ph.D. degrees in communication and information systems from Xidian University, where she is currently a Professor with the School of Telecommunications Engineering. Her research interests include wireless communication systems, cognitive radio networks, and digital signal processing.